

See discussions, stats, and author profiles for this publication at: <https://www.researchgate.net/publication/237055149>

# Density Functional Calculations of the Structural and Electronic Properties of $(Y_2O_3)_n(n=0,+/-1)$ Clusters with $n=1-10$

ARTICLE in THE JOURNAL OF PHYSICAL CHEMISTRY A · JUNE 2013

Impact Factor: 2.69 · DOI: 10.1021/jp404225k · Source: PubMed

---

CITATIONS

6

---

READS

53

## 4 AUTHORS, INCLUDING:



[Amol Rahane](#)

K. T. H. M. College, Nashik, India

9 PUBLICATIONS 48 CITATIONS

[SEE PROFILE](#)



[Mrinalini D. Deshpande](#)

Gokhale Education Society's H.P.T. Arts and ...

20 PUBLICATIONS 243 CITATIONS

[SEE PROFILE](#)



[Vijay Kumar](#)

Dr. Vijay Kumar Foundation

207 PUBLICATIONS 3,907 CITATIONS

[SEE PROFILE](#)

# Density Functional Calculations of the Structural and Electronic Properties of $(Y_2O_3)_n^{0,\pm 1}$ Clusters with $n = 1-10$

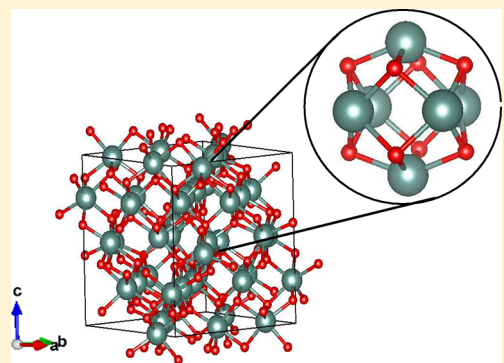
Amol B. Rahane,<sup>†,‡</sup> Punam A. Murkute,<sup>†</sup> Mrinalini D. Deshpande,<sup>\*,†</sup> and Vijay Kumar<sup>§</sup>

<sup>†</sup>Department of Physics, H. P. T. Arts and R. Y. K. Science College, Nasik, Maharashtra 422 005, India

<sup>‡</sup>Department of Physics, University of Pune, Pune, Maharashtra 411 007, India

<sup>\*</sup>Dr. Vijay Kumar Foundation, 1969 Sector 4, Gurgaon 122 001, Haryana, India, and Center for Informatics, Shiv Nadar University, Chithera, Gautam Budh Nagar 203207, Uttar Pradesh, India

**ABSTRACT:** We report results of ab initio calculations on yttrium oxide clusters using a plane wave pseudopotential method within density functional theory.  $(Y_2O_3)_n$  clusters in the size range  $n = 1-10$  prefer compact and symmetric globular configurations where preference for an octahedron unit of  $Y_6O_8$  is seen. The evolution of the atomic structures shows similarity with that of the local structure in the bulk cubic ( $C-Y_2O_3$ ) phase. The maximum coordinations of Y and O atoms are 6 and 4, respectively. The addition (removal) of an electron to (from) the lowest energy configurations of the neutral clusters induces significant changes for some of the cluster sizes. Sequential addition of a  $Y_2O_3$  unit to the  $(Y_2O_3)_n$  cluster leads to an increase in the binding energy. However, the HOMO–LUMO gap, ionization potential, and electron affinity do not show any systematic variation in these clusters with increasing size. The bonding characteristics have been studied using charge density and Bader charge analysis. The charge transfer from Y atoms to oxygens increases with the increase in the cluster size and approaches the value in bulk. The stability of the clusters is dominated by ionic Y–O interactions. However, a small degree of covalency is also seen in Y–O bonding. All the lowest energy configurations of neutral clusters prefer the lowest spin state and the ionic clusters prefer a doublet state.



## 1. INTRODUCTION

Alumina ( $\alpha\text{-Al}_2\text{O}_3$ ) and yttria ( $C\text{-Y}_2\text{O}_3$ ) are the two most important ceramic materials that have wide technological applications ranging from electronics, optics, and mechanical engineering to catalyst support. Between these two stable end crystals, there exist three compounds with different Al to Y ratios:  $\text{Y}_3\text{Al}_5\text{O}_{12}$  (YAG),  $\text{YAlO}_3$  (YAP), and  $\text{Y}_4\text{Al}_2\text{O}_9$  (YAM). They comprise the Y–Al–O system, and all have complex structures with distinct and well-defined local atomic coordinations.<sup>1</sup> Yttrium in its ceramic structures such as YAG and YAP finds applications in optical sensors with high sensitivity or in X-ray detection material. Apart from the ideal spectroscopic properties of the yttrium ions in YAG crystal, low-thermal expansion, high-optical transparency, low-acoustic loss, high threshold for optical damage, hardness, and general stability against chemical and mechanical changes of YAG contribute to its success as the most widely used laser material. It is also known that YAG is one of the most creep resistant oxides and, therefore, has important applications in high-temperature ceramic composites. It has been known that Y has a very low solubility in bulk alumina, but a small addition of Y leads to an increase in adhesion of Al containing oxides.<sup>2–4</sup> Y atoms segregate to the internal grain boundaries (GB) when doped in  $\alpha\text{-Al}_2\text{O}_3$ . This segregation inhibits GB diffusion and increases creep resistance.<sup>5–9</sup> This is the so-called “Y effect”. The microscopic understanding of the Y effect is one of the

most outstanding problems in materials science and technology. Also YAG crystals are doped with rare earths such as Nd or Gd for developing laser materials. A similar problem of segregation of rare earths occurs in YAG and it is difficult to dope rare earths. To understand the segregation effect, clusters of yttrium oxide, aluminum oxide, and mixed phases of Y–Al–O can be used as prototype models because, similar to internal boundaries and surfaces, clusters have a large fraction of atoms exposed to surface where strain can be released by a larger dopant atom. Recently, we have initiated a systematic study to understand the structural and electronic properties of clusters of metal oxides and obtained the equilibrium structures, bonding nature, and other electronic properties of pure alumina as well as Gd doped alumina clusters.<sup>10,11</sup> These studies did show the tendency of Gd to segregate on the surface of alumina clusters. Continuing this effort, in the present study we aim to understand the structural and electronic properties of yttria clusters.

Bulk yttrium oxide exists in cubic  $C\text{-Y}_2\text{O}_3$  (space group  $Ia\bar{3}$ ,  $\text{Mn}_2\text{O}_3$  bixbite type) phase<sup>12</sup> with a wide band gap of 5.8 eV. It has a high melting point ( $T_m$ ), which is higher than that of a number of other well-known oxides such as alumina, zirconia,

**Received:** April 29, 2013

**Revised:** June 4, 2013

**Published:** June 4, 2013

yttriums—aluminum garnet (YAG), and spinel. Yttrium and yttrium oxide clusters have been studied both experimentally and theoretically due to their possible applications.<sup>13–20</sup> Most of these studies restricted to the small size with monomer, dioxide, and trioxide clusters.<sup>17–20</sup> Experimentally, Wu and Wang have studied the electronic structure of small  $\text{YO}_n^-$  clusters with  $n = 1–5$ <sup>13</sup> using photoelectron spectroscopy (PES). Pramann et al. have investigated the PES of  $\text{Y}_n\text{O}_m^-$  clusters with  $n = 2–10$ ,  $m = 1–3$ , and the electron affinities and vertical detachment energies of these species.<sup>14</sup> Recently, Knickelbein calculated IPs of the  $\text{Y}_n$  and  $\text{Y}_n\text{O}$  clusters with  $n = 2–31$ .<sup>15</sup> All the earlier studies considered both metal-excess and oxygen-excess fragments to investigate the effects of the oxygen/metal ratio on their structural and electronic properties. In the present study we perform calculations on stoichiometric  $(\text{Y}_2\text{O}_3)_n$  clusters, with  $n = 1–10$  using the density functional theory (DFT) with plane wave pseudopotential approach. Our aim is to understand the evolution of structural and electronic properties of clusters with the stoichiometry of bulk  $\text{Y}_2\text{O}_3$  and to determine their convergence to the corresponding bulk values. We report here the results on the equilibrium structure, stability and bonding, electron affinity (EA), and ionization potential (IP) of  $(\text{Y}_2\text{O}_3)_n$  clusters. It is seen that the lowest energy configurations of these clusters prefer closed compact structures with an octahedral unit.

The organization of the paper is as follows. Section 2 deals with the computational method used in this work. The results are presented and discussed in section 3. Finally, we present our conclusions in section 4.

## 2. COMPUTATIONAL DETAILS

The calculations have been performed using the Vienna ab initio Simulation Package (VASP)<sup>21,22</sup> with the generalized gradient approximation (GGA) of Perdew, Burke, and Ernzerhof (PBE)<sup>23</sup> for the exchange–correlation functional and projector augmented wave (PAW) pseudopotential method<sup>24,25</sup> for treating the electron–ion interaction. The ionic pseudopotentials have been generated by considering scalar relativistic effects. The valence electronic configuration of the Y (O) atom in the pseudopotential is taken to be  $4s^24p^65s^24d^1$  ( $2s^22p^4$ ). Following our earlier studies on  $\text{Al}_2\text{O}_3$  and  $\text{Ga}_2\text{O}_3$  clusters,<sup>10,11,26</sup> we used a cubic supercell with an edge of 24 Å, which is large enough so that the interaction between the cluster and its periodic images is negligible. The cutoff energy for the plane wave expansion was set to 282.8 eV. The calculations were considered to be converged when the force on each ion was less than 0.001 eV/Å, with a convergence in the total energy of about  $10^{-5}$  eV. Several initial planar and nonplanar atomic configurations were considered for clusters and some of the initial configurations were also taken from our earlier studies on  $\text{Al}_2\text{O}_3$  and  $\text{Ga}_2\text{O}_3$  clusters<sup>10,11,26</sup> as well as by adding oxygen atoms to bare  $\text{Y}_n$  clusters.<sup>27,28</sup> The stability of the cluster is further verified by performing spin-polarized calculations with different spin states. The structural symmetry is determined using VMD package.<sup>29</sup>

Calculations have also been performed on bulk C- $\text{Y}_2\text{O}_3$  with VASP by keeping the same exchange–correlation functional and energy cutoff as for the cluster calculations. The unit cell of bulk yttria consist of sixteen  $\text{Y}_2\text{O}_3$  units (Figure 1). We use  $4 \times 4 \times 4$  Monkhorst–Pack<sup>30</sup> k-point sampling for Brillouin zone integrations. The calculated lattice parameter  $a = 10.637$  Å within GGA-PBE is in very good agreement with the experimental value of 10.604 Å by Paton et al.,<sup>12</sup> and slightly

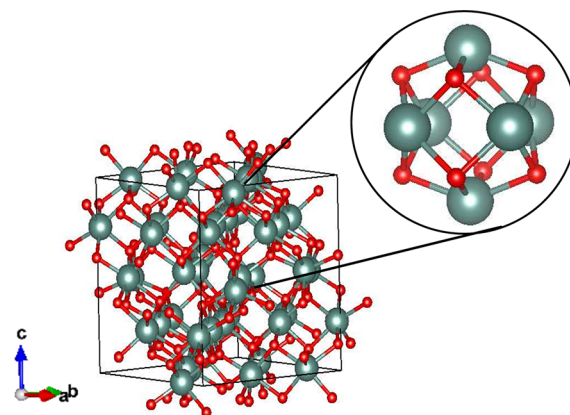


Figure 1. Supercell of bulk C- $\text{Y}_2\text{O}_3$  along with a  $\text{Y}_6\text{O}_8$  fragment.

lower than 10.759 Å obtained by Halevy et al.<sup>31</sup> Our results are also in agreement with another experimental result of 10.603 Å by Riello et al.<sup>32</sup> using X-ray Rietveld analysis and theoretical calculations (10.598 Å) by Belonoshko et al.<sup>33</sup> using full potential linearized augmented plane wave (FPLAPW) method. The calculated cohesive energy for C- $\text{Y}_2\text{O}_3$  is 7.304 eV/atom. In the bulk phase, all the Y atoms have octahedral coordination whereas O atoms prefer tetrahedral coordination. The Y–O bond lengths are in the range 2.25–2.34 Å, which are consistent with the earlier studies.<sup>34–38</sup>

## 3. RESULTS AND DISCUSSION

Before beginning our discussion, we note that the calculated binding energy (BE) and bond length (BL) of YO dimer are 3.70 eV and 1.83 Å, respectively. On the other hand, the calculated BE of  $\text{Y}_2$  and  $\text{O}_2$  is 1.59 and 6.10 eV whereas the BL is 2.9 and 1.29 Å, respectively. Our results of the BL of  $\text{Y}_2$  agree well with the earlier results<sup>28,39</sup> of 2.95–3.03 Å but the BE is underestimated compared with the values<sup>28,39</sup> 2.16–2.56 eV. Further, the BE of the YO dimer (3.70 eV) is much larger than 1.59 eV for  $\text{Y}_2$  whereas the BL of YO is 1.83 Å compared with 2.9 Å for  $\text{Y}_2$ . Therefore, there is a preference for the formation of Y–O bonds over Y–Y bonds. However, compared to that of two YO dimers,  $\text{Y}_2$  and  $\text{O}_2$  are slightly more stable. This, however, changes when  $\text{Y}_2\text{O}_3$  clusters are considered. The calculated magnetic moments for  $\text{Y}_2$ ,  $\text{O}_2$ , and YO dimers are 4, 2, and 1  $\mu\text{B}$ , respectively.

The lowest energy atomic structures, as well as a few low-lying isomers for each size of  $(\text{Y}_2\text{O}_3)_n$  ( $n = 1–10$ ) clusters, are shown in Figures 2 and 3. An analysis of the atomic structures shows that the lowest energy configurations evolve with an octahedral unit of  $\text{Y}_6\text{O}_8$  and there is a preference for the formation of Y–O bonds over Y–Y and O–O bonds. For  $n = 1$ , we find that the lowest energy configuration of  $\text{Y}_2\text{O}_3$  is a three-dimensional (3D) symmetric trigonal bipyramidal with  $D_{3h}$  symmetry and it has a singlet spin state. The triplet spin state is 2.22 eV higher in energy than the singlet state. All the Y–O bond distances in the singlet configuration are 2.08 Å, whereas the two Y atoms are separated by 2.75 Å. The BE is 5.59 eV/atom, which is much higher than the value for a YO dimer. The 3D-kite configuration with a terminal oxygen is 1.26 eV higher in energy than the 3D configuration. Three more isomers including planar and linear structures, shown in Figure 2 lie much higher in energy. The preference for the 3D structure is due to the involvement of the Y-4d orbitals in bonding. Our results for the  $\text{Y}_2\text{O}_3$  cluster are in agreement with the previous

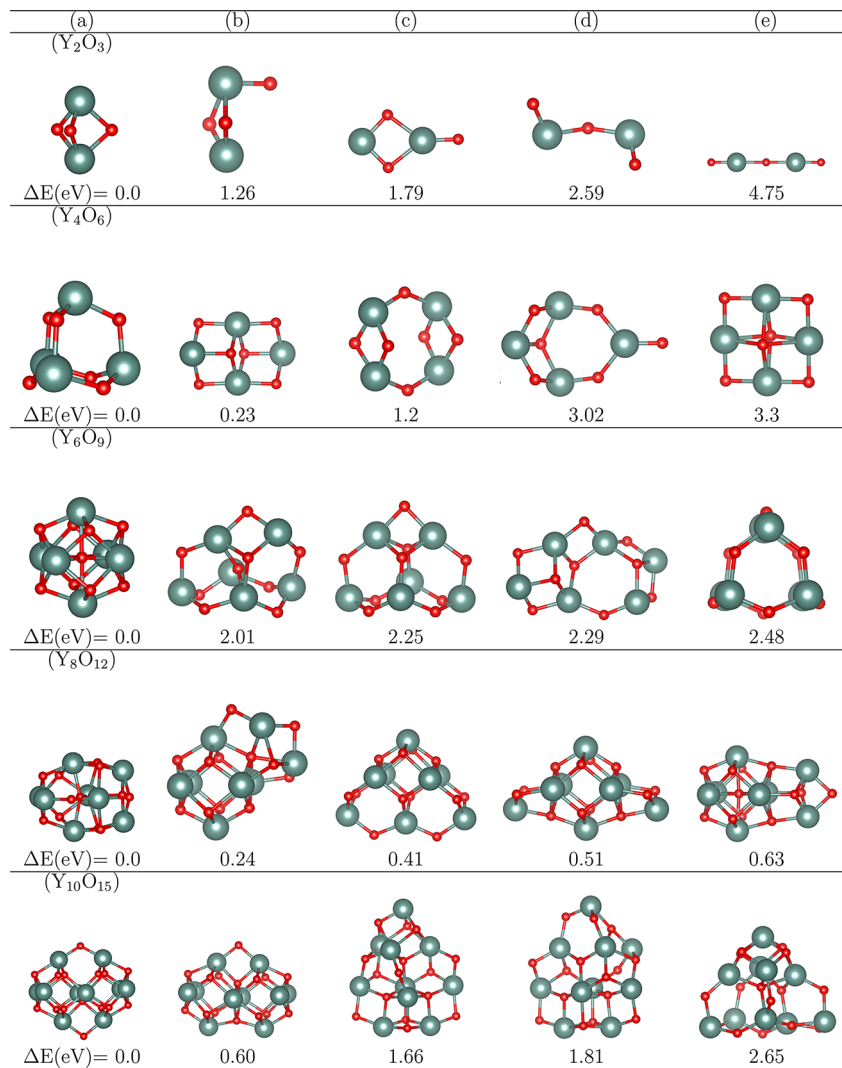


**Figure 2.** Atomic structures of the lowest energy and some of the low-lying isomers of  $(Y_2O_3)_n$  clusters with  $n = 1–5$ . Blue (red) spheres represent Y (O) atoms. The energy of an isomer is given with respect to the energy (taken to be zero) of the lowest energy isomer for a given size.

theoretical studies.<sup>16,20</sup> For  $n = 2$ , in the lowest energy configuration of  $(Y_2O_3)_2$ , all the Y atoms form a regular tetrahedron and six O atoms cap the edges of the tetrahedron to have a structure with  $T_d$  symmetry. In this configuration, all the Y atoms are 3-fold coordinated and O atoms have 2-fold coordination. All the Y–O bond distances are 2.07 Å. Another isomer with 3D capped-windowpane configuration is only 0.23 eV higher in energy than the lowest energy configuration. A few other isomers we studied lie more than 1 eV higher in energy than the lowest energy isomer.

For  $n = 3$ , the six Y atoms form a regular octahedron ( $O_h$ ) in the lowest energy configuration and one oxygen atom is at the center whereas eight oxygen atoms cap the eight faces of the octahedron. In this configuration all the Y atoms have 5-fold coordination whereas the central oxygen is 6-fold coordinated. The rest of the O atoms have 3-fold coordination. All the Y–O bond distances are 2.23 Å. The increase in the Y–O bond distances compared with the values for the  $n = 2$  cluster is due to the increase in the average coordination of atoms in this cluster. Interestingly, one can also see an octahedral unit for  $n = 3$  without the central oxygen, i.e.,  $Y_6O_8$ . This unit is also found as the structural motif in the bulk C- $Y_2O_3$  structure (Figure 1).

In the size range  $n = 4–10$ , several initial structures, both ordered and disordered, were considered. It is noted that with the successive addition of the  $Y_2O_3$  unit, the clusters evolve around the octahedron configuration of  $Y_6O_8$ . A few other configurations including caged isomers lie quite high in energy and suggest high stability of the octahedral cluster. For  $n = 4$ , the lowest energy structure evolves from the lowest energy structure of  $Y_6O_9$  with the minimum Y–O bond distance of 2.02 Å. In this configuration, one of the Y atoms is 6-fold coordinated. A few other isomers derived primarily from the octahedral isomer of  $n = 3$  lie 0.21–0.63 eV higher in energy than the lowest energy isomer. For  $n = 5$ , the lowest energy configuration ( $C_{2v}$ ) consists of two units of  $Y_6O_8$ . Another similar isomer with a slight change in O position lies 0.60 eV higher in energy whereas a few other isomers without an octahedral unit lie significantly higher in energy. For  $n = 6$ , the lowest energy structure is a three-layered ( $C_s$ ) configuration. There are two O atoms inside the cage structure. The minimum Y–O bond distance is 2.04 Å whereas the maximum coordination of Y atom and O atom is 6. The caged dimer configuration ( $D_{2d}$ ), which is a combination of two  $Y_6O_9$  octahedral units ((6c) in Figure 3) connected via four Y–O bonds, is 0.18 eV higher in energy. In this configuration, four Y

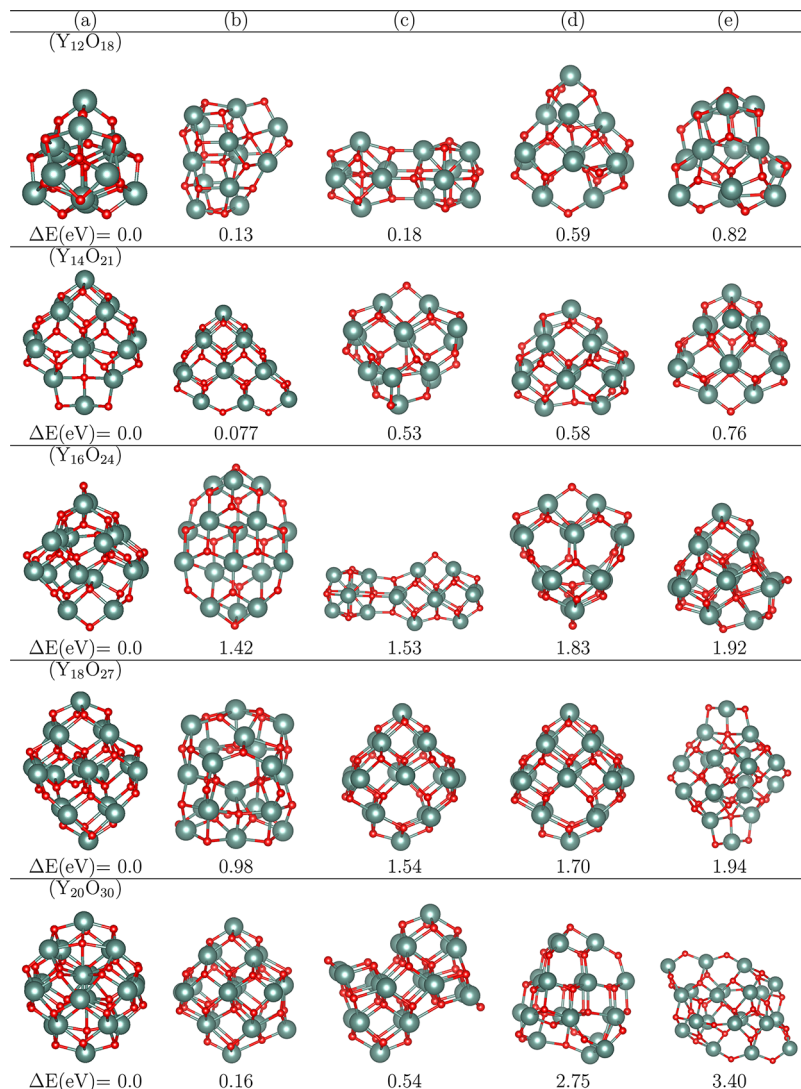


**Figure 3.** Atomic structures of the lowest energy and some of the low-lying configurations for  $(\text{Y}_2\text{O}_3)_n$  clusters with  $n = 6–10$ . Other details are the same as in Figure 2.

atoms are 6-fold coordinated, and two O atoms are 4-fold coordinated with the minimum Y–O bond distance of 2.20 Å. A few other isomers are also shown in Figure 3, and these results show that with increasing size more isomers compete in energy.

The lowest energy isomers for the clusters with  $n = 7–9$  are multilayered symmetric configurations. For  $(\text{Y}_2\text{O}_3)_7$ , a layered configuration with  $C_s$  symmetry has the lowest energy. There is one 4-fold coordinated O atom inside the cluster. Another isomer with a slightly different capping of a  $\text{YO}_2$  unit lies close in energy (only 0.077 eV higher) whereas a few other isomers are about 0.5 eV higher in energy. The addition of  $\text{Y}_2\text{O}_3$  unit to  $(\text{Y}_2\text{O}_3)_7$  favors a  $C_3$  symmetric, three-layered distorted pyramidal configuration for  $n = 8$ . There are six tetrahedrally coordinated O atoms inside the cage of Y atoms. One of the low-lying configurations for  $n = 8$  ((8d) in Figure 3) is derived by adding a  $\text{Y}_2\text{O}_3$  unit in one of the isomers ((7e) in Figure 3) of the  $(\text{Y}_2\text{O}_3)_7$  cluster. Further addition of a  $\text{Y}_2\text{O}_3$  unit to this isomer leads to the lowest energy configuration ( $C_s$ ) of  $(\text{Y}_2\text{O}_3)_9$ . In this configuration for  $n = 9$ , one of the octahedrally coordinated Y atoms is inside the cage. For the cases of  $n = 8$  and 9, other isomers lie much higher in energy.

For the  $n = 10$  cluster, a highly symmetric globular configuration ( $D_{3d}$ ) is found to be of the lowest energy. In this configuration, six Y atoms form a regular octahedron, twelve Y atoms are at the edges of the octahedron, and two Y atoms are inside the octahedron. The oxygen atoms prefer the capping sites between Y atoms. This increases their coordination with the Y atoms. Six Y atoms are 4-fold coordinated, twelve are 5-fold coordinated, and two Y atoms at the centers have 6-fold (octahedral) coordination. Note that, in bulk  $\text{C-Y}_2\text{O}_3$ , the coordination for all the Y atoms is 6 whereas all the O atoms are 4-fold coordinated. Another similar isomer lies only 0.16 eV higher in energy. It has a layered structure. Another isomer with layered structure lies 0.54 eV higher in energy (10d and 10e in Figure 3). Two other isomers with much higher energy are also shown.

Overall, for yttrium oxide clusters with bulk stoichiometry  $(\text{Y}_2\text{O}_3)_n$ , in the size range  $n = 1–10$ , we find that the clusters prefer symmetric globular configurations. The lowest energy configurations of clusters with  $n \geq 4$  favor structures that evolve around a bulk derived octahedron configuration of  $\text{Y}_6\text{O}_8$ . The globular structures evolve as the number of  $\text{Y}_6\text{O}_8$  units increases. From  $n = 4$ , in the lowest energy configuration, the

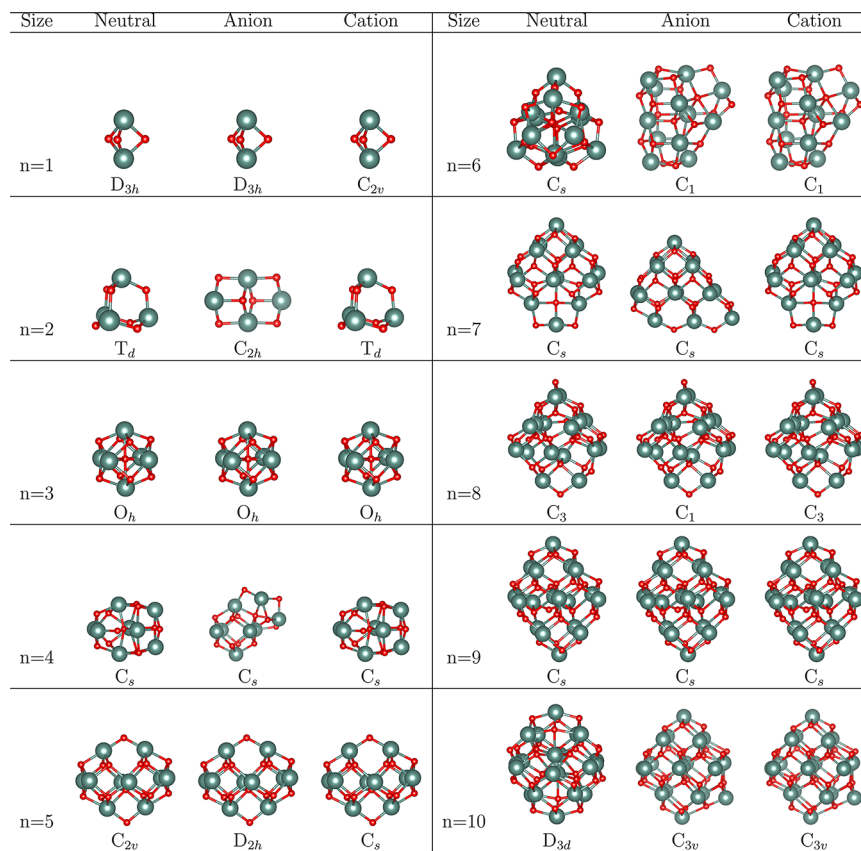


**Figure 4.** Lowest energy configurations of the neutral and ionic  $(Y_2O_3)_n$  clusters with  $n = 1-10$  along with their structural symmetry. Other details are same as in Figure 2.

maximum coordination of Y atoms increases to 6. For  $n = 3$ , the maximum coordination number of the O atom is 6 for the central O within the octahedral unit. However, most of the O atoms in the large size clusters are 3-fold and 4-fold coordinated. Therefore, the  $n = 3$  cluster is special with an O atom having 6-coordination. All the lowest energy configurations of these clusters in this size range prefer the lowest spin state.

Yuan et al.<sup>28</sup> studied  $Y_n$  clusters in the size range  $n = 2-17$ , and Zhao et al.<sup>27</sup> have studied  $Y_n$  and  $Y_nAl$  clusters in the size range  $n = 1-14$ .  $Y_n$  clusters favor compact structures with icosahedral growth pattern showing large magnetic moments. It is interesting to compare the behavior of  $Y_2O_3$  clusters with that of the bare  $Y_n$  clusters where  $n$  is an even integer. It can be seen that for  $Y_{2n}O_{3n}$  clusters ( $n = 1-4$ ), the removal of oxygen atoms lead to the same geometric arrangement (longer bond lengths) of yttrium atoms as that of the bare  $Y_{2n}$  clusters. Therefore, in a way one can also consider the yttria clusters to evolve from the oxidation of yttrium clusters.

Yttrium is trivalent and forms  $Y_2O_3$  oxide similar to the oxides of Al, In, and Ga. Earlier,<sup>10,26</sup> we have studied the structural and electronic properties of  $(Al_2O_3)_n$  and  $(Ga_2O_3)_n$  clusters in the same size range. The comparison with those results show that  $Y_2O_3$  clusters prefer more symmetric and globular configurations than those of  $Al_2O_3$  and  $Ga_2O_3$  clusters. It is also seen that  $Y_2O_3$  clusters approach bulk-like behavior at much smaller size compared with those of aluminum and gallium oxide clusters. Furthermore, yttrium and lanthanum are in the same column of the periodic table. Ding et al.,<sup>40</sup> have studied the structural and electronic properties of  $(La_2O_3)_n$

clusters in the size range  $n = 1-6$  using evolutionary algorithm. Similarly to  $Y_2O_3$ ,  $La_2O_3$  clusters also favor globular structures and approach the bulk structure at remarkably small cluster size.

To study the charge induced changes in the structure and electronic properties of the clusters, we considered the lowest and some of the low-lying configurations of  $(Y_2O_3)_n$  clusters. The optimized lowest energy configurations for the neutral and ionic configurations are shown in Figure 4. It is found that in ionic clusters, the addition (removal) of an electron to (from) the neutral cluster induces significant changes for some of the cluster sizes. The atomic structures of the cationic lowest energy isomers remain similar to those of the neutral clusters except for  $n = 6$  and 10. For the anionic clusters, the lowest energy configurations for  $n = 2, 4, 6, 7$ , and 10 are different from those of the neutral configurations. The Bader charge analysis for the lowest energy and some of the low-lying configurations of the ionic clusters shows that the additional electron is mainly located on the oxygen atoms and is distributed in their p-orbitals. This results in enhancement of the Y–O bond lengths by about 2–3% compared with the neutral cluster. For the cationic clusters, the electron is mainly removed from the hybridized 4d and 5s orbitals of Y atoms. This results in a shortening of the Y–O bond lengths by about 1% as compared to those of the neutral cluster. The anionic and cationic configurations have a doublet spin state.

For  $n = 2$ , the bicapped windowpane isomer with  $C_{2h}$  symmetry (2(b) in Figure 2) has the lowest energy for the anionic case. This isomer is nearly degenerate ( $\Delta E = 0.08$  eV) with the isomer obtained from the neutral lowest energy isomer

( $T_d$ ). For  $n = 4$ , the addition of an electron distorts the lowest energy configuration significantly. The isomer 4(b) in Figure 2 is at the lowest energy for the anionic case. The isomer obtained from the lowest energy isomer 4(a) in the neutral case is 0.12 eV higher in energy. For  $n = 6$ , the isomer 6(b) in Figure 2 is at the lowest energy for both the anionic and cationic configurations. For the anion of  $n = 6$ , the isomer 6(a) obtained from the neutral lowest energy isomer is 0.17 eV higher in energy, whereas for the cationic case it is nearly degenerate ( $\Delta E = 0.015$  eV). For  $n = 7$ , for the anionic case the isomer 7(b) with  $C_s$  symmetry is at the lowest energy. The isomer obtained from the neutral lowest energy isomer (7a) is nearly degenerate (0.08 eV) to the isomer obtained from 7(b). For  $n = 10$ , the anionic and cationic configurations are different from the neutral case. The isomer with  $C_{3v}$  symmetry (10(b)) in Figure 2 has the lowest energy for both the cationic and anionic configurations. The addition or removal of an electron moves one of the central 6-fold coordinated Y atom toward the surface of the cluster and the coordination of this Y atom becomes 3. The Y–O bond distances for the neutral clusters are in the range 2.02–2.23 Å, and those of the anionic and cationic clusters are in the range 2.06–2.32 and 2.00–2.32 Å, respectively.

The stability of the neutral and ionic clusters can be discussed on the basis of the binding energy per atom (BE) and the fragmentation energy. The BE is calculated as

$$E_b[(Y_2O_3)_n] = (-E[(Y_2O_3)_n] + 2nE[Y] + 3nE[O])/(5n) \quad (1)$$

where  $E$  is the total energy of the system.

The BE for  $(Y_2O_3)_n$  clusters is shown in Figure 5. Also the variation in the average number of the nearest neighbors of Y

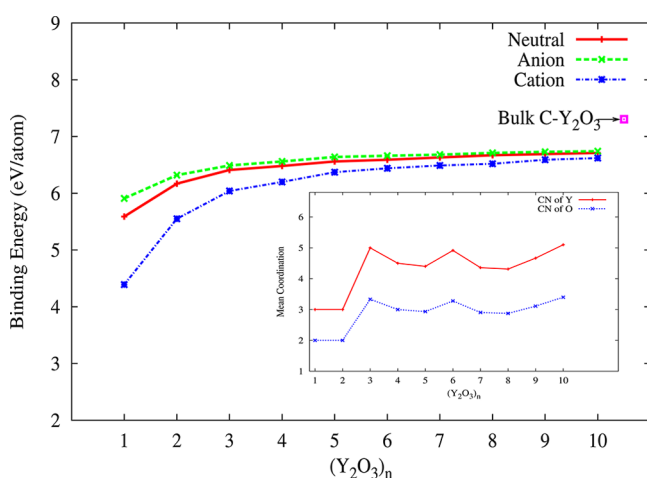


**Figure 5.** Binding energy for the lowest energy isomers of  $(Y_2O_3)_n$  clusters with  $n = 1-10$ . The calculated bulk cohesive energy (eV/atom) for C- $Y_2O_3$  is also shown by a pink square with an arrow. The inset shows the average coordination number (CN) for Y and O atoms in the lowest energy configurations of yttria clusters with  $n = 1-10$ .

and O atoms in the lowest energy isomers are shown in the inset. With successive addition of a  $Y_2O_3$  unit, there is an increase in the BE and the average coordination of Y and O atoms. The average coordination is maximum for  $n = 3$  and 6. There is a decrease at  $n = 7$  and again it increases with  $n$  up to 10. The increase in the coordination number corresponds to the formation of the layered structures. As noted earlier, with the increase in size, some of the Y atoms prefer coordination

with six oxygen atoms and oxygen atoms are tetrahedrally coordinated. Note that the average coordination for bulk C- $Y_2O_3$  is 6 for Y atoms. We have also calculated the BE per  $Y_2O_3$  for all the clusters. For  $n = 10$ , the BE per  $Y_2O_3$  is 33.55 eV, which is lower than the calculated cohesive energy for C- $Y_2O_3$  (36.52 eV). It is observed that the lowest energy configurations for these clusters prefer geometries which are derived from bulk configuration. The preference for octahedron  $Y_6O_8$  is seen in the lowest energy configurations. However, due to the reduced coordination in clusters, the BE energy is lower than the cohesive energy of the bulk phase.

Further, the stability of the clusters is also analyzed by calculating their fragmentation energy (FE). The FE with respect to the loss of a  $Y_2O_3$  unit is calculated as

$$\begin{aligned} \Delta E[(Y_2O_3)_n] = & -E[(Y_2O_3)_n] + E[(Y_2O_3)_{(n-1)}] \\ & + E[(Y_2O_3)] \end{aligned} \quad (2)$$

where  $E$  is the total energy of the system. The FEs for  $(Y_2O_3)_n$  clusters,  $n = 2-10$ , associated with the loss of a  $(Y_2O_3)$  unit are 5.81, 6.52, 5.40, 6.63, 5.75, 6.36, 5.90, 5.55, and 7.99 eV, respectively. It indicates that the FE has an oscillatory behavior with a high FE value for clusters having odd  $n$  (except for  $n = 9$ ) compared with those with even  $n$ . Interestingly, the highest FE value is obtained for the cluster with  $n = 10$ .

The calculated EA and IP are presented in Table 1. The vertical and adiabatic EAs and IPs give the indication of the relative stability of the neutral and ionic clusters. The vertical detachment energy (VDE) is defined as the energy difference between the anionic and neutral clusters with both at the optimized geometry of the anionic cluster, whereas the vertical attachment energy (VAE) or vertical electron affinity (VEA) is defined as the energy difference between the anionic and neutral clusters with both at the optimized geometry of the neutral cluster. Adiabatic electron affinity (AEA) is defined as the energy difference between the anionic and neutral clusters at their own respective optimized geometries. Similarly, the vertical ionization potential (VIP) is defined as the energy difference between the cationic and neutral clusters with both at the optimized geometry of the neutral cluster, whereas the adiabatic ionization potential (AIP) is defined as the energy difference between the cationic and neutral clusters at their own respective optimized geometries.<sup>41,42</sup>

Yang et al.<sup>20</sup> calculated the IPs and EAs for  $Y_2O_3$  clusters using Slater-type-orbital (STO) basis sets and triple- $\zeta$  plus polarization functions (TZ2P) within DFT. Their calculated values of IP and EA for  $Y_2O_3$  are 6.7 and 1.1 eV, respectively. Our values of IP (EA) for  $Y_2O_3$  are slightly lower (higher) compared to the previous study. According to Table 1, the computed EA and IP values do not show any systematic variation in going from  $n = 1$  to 10. The values of EAs and IPs show an oscillatory behavior with increasing  $n$ . Overall, there is a decreasing (increasing) trend in the values of IP (EA) with increasing  $n$ . For the clusters where there is not much topological difference between neutral and ionic configurations of the  $(Y_2O_3)_n$  clusters, the vertical and adiabatic values of EAs and IPs are nearly similar. For cationic clusters with  $n = 6$  and 10, and anionic clusters with  $n = 2, 4, 6, 7, 8$ , and 10, the differences in the AEA and VEA values are due to topological variations in the ground state configurations in their neutral and charged states.

The calculated highest occupied molecular orbital–lowest unoccupied molecular orbital (HOMO–LUMO) gaps for the

**Table 1.** Adiabatic Ionization Potential (AIP), Vertical Ionization Potential (VIP), Adiabatic Electron Affinity (AEA), Vertical Electron Affinity (VEA) or Vertical Attachment Energy (VAE), Vertical Detachment Energy (VDE) and Fundamental Gap for  $(Y_2O_3)_n$  Clusters with  $n = 1\text{--}10$  (in eV)

system	1	2	3	4	5	6	7	8	9	10
AIP	5.98	5.90	5.55	5.01	4.92	5.78	4.96	5.31	4.58	4.46
VIP	5.98	5.99	5.55	5.21	4.93	4.79	4.97	5.31	4.59	4.68
AEA	1.54	1.49	1.17	1.63	1.73	1.71	1.70	2.19	1.69	2.16
VEA(VAE)	1.52	1.37	1.16	1.47	1.69	1.49	1.57	1.96	1.68	1.38
VDE	1.55	1.75	1.17	1.99	1.76	1.95	2.00	2.55	1.76	2.81
fundamental gap VIP-VEA	4.46	4.62	4.39	3.74	3.24	3.30	3.40	3.35	2.91	3.30

neutral and ionic  $(Y_2O_3)_n$ ,  $n = 1\text{--}10$ , clusters are presented in Figure 6. The neutral clusters show a higher value of the

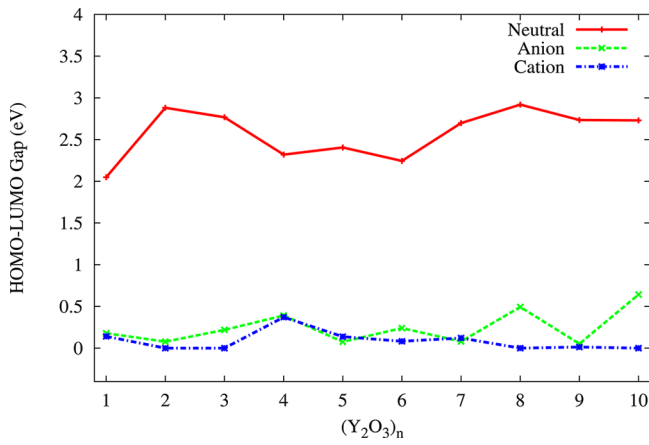


**Figure 6.** HOMO–LUMO gap for the lowest energy configurations of neutral and ionic  $(Y_2O_3)_n$  clusters with  $n = 1\text{--}10$ .

HOMO–LUMO gap than the anionic or cationic clusters. The HOMO–LUMO gap for the neutral lowest energy configurations varies in the range 2.04–2.88 eV. For  $n = 10$ , in the ionic case there is a significant variation in the cluster symmetry and it reduces the HOMO–LUMO gap of the cationic cluster and enhances the HOMO–LUMO gap for the anionic cluster compared to the smaller size clusters. For the sake of comparison, we have also calculated the band gap for bulk C– $Y_2O_3$ . The calculated band gap at the  $\Gamma$ -point is 4.15 eV. For  $n = 10$ , the HOMO–LUMO gap is 2.73 eV, which is much lower than the bulk value. The smaller value in clusters is due to the lower coordination of O atoms that makes some of the O-p states lie close to the HOMO. Note that the experimental band gap for the bulk C– $Y_2O_3$  is 5.8 eV. The underestimation of the calculated values of the bulk band gap is due to the use of GGA.<sup>10,26</sup> The same is also true for clusters. The fundamental gap of the molecule is defined as the difference between the molecular VIP and the VEA. The calculated fundamental gap of these clusters is presented in Table 1. It is seen that the calculated HOMO–LUMO gap is significantly lower than the fundamental gap of a cluster.

In bulk  $Y_2O_3$ , the bonding is mainly ionic. To understand the nature of bonding in clusters, we have calculated the charge density, total density of states (DOS), and site projected DOS (PDOS) for Y and O atoms for these clusters. As a representative, we have shown in Figure 7 the total DOS and the site PDOS along with the charge density contours for the lowest energy configurations of  $Y_6O_9$  and  $Y_{20}O_{30}$  clusters. For

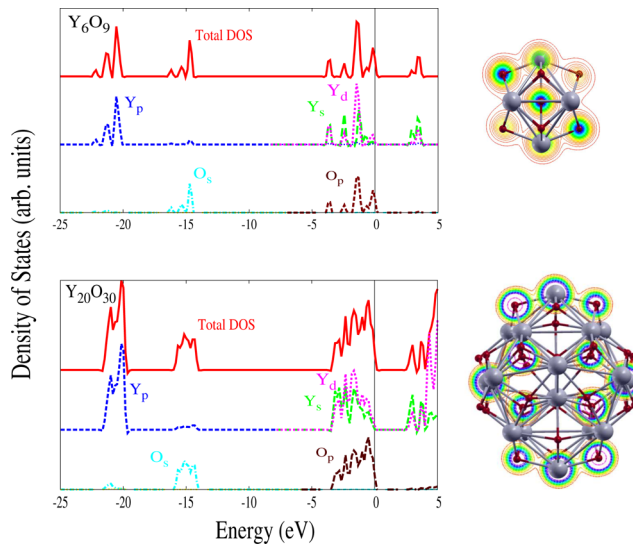


**Figure 7.** Total and site projected density of states (DOS) along with the charge density contours for the lowest energy configurations for  $Y_6O_9$  and  $Y_{20}O_{30}$  clusters. The HOMO is aligned to zero.

the small size with  $n = 3$ , the spectra show sharp peaks but with the increase in cluster size ( $n = 10$ ), the DOS spectrum becomes broader. The Y-4s states lie at much lower energies and hence are not shown in Figure 7. The Y-4p states are observed in the lower energy part of the spectra. The middle energy part of the spectra is dominated by 2s orbitals of oxygen atoms. The states near the HOMO consist of the hybridized 5s and 4d states of the Y atoms along with the O-2p states. The 4d electrons of Y atoms play a significant role in the interatomic bonding in these clusters. The HOMO of  $Y_6O_9$  cluster is mainly composed of O-2p orbitals. The LUMO of  $Y_6O_9$  is mainly composed of Y-5s orbitals.

The charge density analysis shows that the bonding between Y and O atoms in  $Y_2O_3$  clusters is also predominantly ionic. From the contour plots for the total charge density (Figure 7), a signature of small covalent character in the Y–O bonding can be noticed. This covalent character decreases with the increase in the cluster size. To better understand the nature of bonding, we have calculated Bader<sup>43</sup> charges for some of the lowest and low-lying configurations of  $(Y_2O_3)_n$  clusters. The charges on Y are relatively higher and indicate the ionic nature of the bonds. For  $n = 1$ , the charge transfer analysis shows that each tricoordinated Y atom in  $Y_2O_3$  gives 1.82e charge to the surrounding O atoms, whereas each oxygen atom takes 1.19e–1.23e charge from the two Y atoms. With the increase in the cluster size, the charge transfer increases. For  $n = 2$ , each tricoordinated Y atom gives nearly 1.98e, whereas each

bicoordinated O atom takes nearly 1.32e charge. For  $n = 3$ , the average charge transfer from the Y atoms increases further and it is around 2.02e to the surrounding oxygen atoms. Here all the tricoordinated oxygen on the edges take around 1.32–1.36e charge from the Y atoms, whereas the central 6-fold coordinated oxygen atom takes only 1.28e charge from Y atoms. In these clusters the charge transfer from Y atom to O atom increases with the increase in cluster size as well as with the increase in the coordination of Y atoms. For  $n = 10$ , the charge transfer from 4-fold coordinated Y atom is in the range 1.95e–2.12e, whereas from 5-fold coordinated Y atoms it is in the range 2.02e–2.04e and that from 6-fold coordinated Y atoms it is in the range 2.12e–2.14e. The charge taken by 3-fold coordinated O atoms is in the range 1.33e–1.40e, and that of the 4-fold coordinated O atoms is in the range 1.34e–1.39e. For comparison, we have also calculated the Bader charges for the bulk cubic phase and the charge on all the Y atoms is +2.12e and on all the O atoms it is −1.41e. Note that the amount of charge transfer from Y to O is in the range 1.95e–2.14e for  $n = 10$ , which is comparable to that of C-Y<sub>2</sub>O<sub>3</sub>.

A small covalent character in the Y–O bonding in crystalline Y<sub>2</sub>O<sub>3</sub> as well as Y doped  $\alpha$ -Al<sub>2</sub>O<sub>3</sub> is reported by Ching et al.<sup>36,44</sup> They have described the yttrium oxide compound with the configuration Y<sub>2</sub><sup>2.16+</sup>O<sub>3</sub><sup>1.44-</sup> rather than Y<sub>2</sub><sup>3+</sup>O<sub>3</sub><sup>2-</sup>. These values can be compared with the Bader charge transfer in (Y<sub>2</sub>O<sub>3</sub>)<sub>n</sub> clusters. In these clusters in the size range we have studied, it is seen that the maximum charge transfer from Y atom to O atom is around 2.14e and the charge gain by oxygen atom is around 1.41e. A small degree of covalency in the bonding associated with reduced coordination is also reported for other metal oxide systems such as Al<sub>2</sub>O<sub>3</sub> and Ga<sub>2</sub>O<sub>3</sub>.<sup>10,26</sup>

We have also compared the Bader charges on Al and O atoms in Al<sub>2</sub>O<sub>3</sub> clusters<sup>10</sup> and Ga and O atoms in Ga<sub>2</sub>O<sub>3</sub> clusters<sup>26</sup> with that of Y and O atoms in Y<sub>2</sub>O<sub>3</sub> clusters. In Al<sub>2</sub>O<sub>3</sub> clusters, the maximum charge transfer from Al to surrounding O atoms is around 2.46e whereas the maximum charge gain by oxygen atoms is around 1.66e. In Ga<sub>2</sub>O<sub>3</sub> clusters, the maximum charge given by Ga atom to surrounding O atoms is around 1.66e whereas the maximum charge gain by oxygen atoms is around 1.18e. From the nature of the Bader charges in these systems, it is seen that the ionicity decreases in going from Al–O → Y–O → Ga–O bond.

#### 4. CONCLUSIONS

We have studied the structural and electronic properties of (Y<sub>2</sub>O<sub>3</sub>)<sub>n</sub> clusters with  $n = 1$ –10 using density functional theory. It is found that these clusters prefer compact and symmetric globular configurations. The lowest energy configuration appears to be derived from the bulk cubic C-Y<sub>2</sub>O<sub>3</sub> structure. The maximum coordination of Y and O atoms in these clusters is 6 and 4, respectively. These are also the values for the bulk phase. The neutral clusters prefer the singlet state whereas ionic clusters prefer the doublet spin state. The BE of the clusters increases with the cluster size. However, it is still lower than the bulk cohesive energy. The stability of the clusters is dominated by ionic Y–O interactions, but Bader charge analysis suggests that there is also significant covalent contribution to bonding. With the increase in the cluster size, the HOMO–LUMO gap remains nearly the same in the size range we have studied, whereas EAs and IPs do not show any systematic variation. We hope that the present work would be a good starting point for understanding further the properties of yttrium oxide clusters and Y–O nanophase materials as well as the effects of dopants.

#### ■ AUTHOR INFORMATION

##### Corresponding Author

\*E-mail: d\_mrinal@yahoo.com.

##### Notes

The authors declare no competing financial interest.

#### ■ ACKNOWLEDGMENTS

A.B.R. and M.D.D. gratefully acknowledge financial assistance from the Department of Science and Technology (DST), Government of India, University Grants Commission (UGC), and Council for Scientific and Industrial Research (CSIR), New Delhi. We also acknowledge the Center for Development of Advance Computing (CDAC), Pune and Bangalore, for providing the supercomputing facilities. V.K. acknowledges support from Asian Office of Aerospace Research and Development.

#### ■ REFERENCES

- (1) Ching, W.-Y.; Xu, Y.-N. Nonscalability and Nontransferability in the Electronic Properties of the Y-Al-O System. *Phys. Rev. B* **1999**, *59*, 12815–12821.
- (2) Przybylski, K.; Yurek, G. J. Segregation of Y to Grain-Boundaries in Cr<sub>2</sub>O<sub>3</sub> and Al<sub>2</sub>O<sub>3</sub> Scales. *J. Electrochem. Soc.* **1987**, *134*, C469.
- (3) Raj, R. Fundamental Research in Structural Ceramics for Service Near 2000 °C. *J. Am. Ceram. Soc.* **1993**, *76*, 2147–2174.
- (4) Lartique, S.; Carry, C.; Priester, L. Grain Boundaries in High Temperature Deformation of Yttria and Magnesia Co-Doped Alumina. *J. Phys. (Paris)* **1990**, *C1*–51, 985.
- (5) French, J. D.; Zhao, J.; Harmer, M. P.; Chan, H. M.; Miller, G. A. Creep of Duplex Microstructures. *J. Am. Ceram. Soc.* **1994**, *77*, 2857–2865.
- (6) Thompson, A. M.; Soni, K. K.; Chan, H. M.; Harmer, Williams, D. B.; Chabala, J. M.; Levi-Setti, R. Dopant Distributions in Rare-Earth-Doped Alumina. *J. Am. Ceram. Soc.* **1997**, *80*, 373–376.
- (7) Gruffel, P.; Carry, C. Effect of Grain Size on Yttrium Grain Boundary Segregation in Fine-Grained Alumina. *J. Eur. Ceram. Soc.* **1993**, *11*, 189–199.
- (8) Loudjani, A. K.; Roy, J.; Huntz, A. M. Study by Extended X-Ray Absorption Fine-Structure Technique and Microscopy of the Chemical-State of Yttrium in Alpha-Polycrystalline Alumina. *J. Am. Ceram. Soc.* **1985**, *68*, 559–562.
- (9) Cho, J.; Chan, H. M.; Harmer, M. P.; Rickman, J. M. Influence of Yttrium Doping on Grain Misorientation in Aluminum Oxide. *J. Am. Ceram. Soc.* **1998**, *81*, 3001–3004.
- (10) Rahane, A. B.; Deshpande, M. D.; Kumar, V. Structural and Electronic Properties of (Al<sub>2</sub>O<sub>3</sub>)<sub>n</sub> Clusters with  $n = 1$ –10 from First Principles Calculations. *J. Phys. Chem. C* **2011**, *115*, 18111–18121.
- (11) Rahane, A. B.; Deshpande, M. D.; Kumar, V. First Principles Calculations for Structural, Electronic, and Magnetic Properties of Gadolinium-Doped Alumina Clusters. *J. Phys. Chem. C* **2012**, *116*, 6115–6126.
- (12) Paton, M. G.; Maslen, E. N. A Refinement of the Crystal Structure of Yttria. *Acta Crystallogr.* **1965**, *19*, 307–310.
- (13) Wu, H.; Wang, L. Photoelectron Spectroscopy and Electronic Structure of ScO<sub>n</sub><sup>−</sup> ( $n = 1$ –4) and YO<sub>n</sub><sup>−</sup> ( $n = 1$ –5): Strong Electron Correlation Effects in ScO<sup>−</sup> and YO<sup>−</sup>. *J. Phys. Chem. A* **1998**, *102*, 9129–9135.
- (14) Pramann, A.; Nakamura, Y.; Nakajima, A.; Kaya, K. Photoelectron Spectroscopy of Yttrium Oxide Cluster Anions: Effects of Oxygen and Metal Atom Addition. *J. Phys. Chem. A* **2001**, *105*, 7534–7540.
- (15) Knickelbein, M. Photoionization Spectroscopy of Yttrium Clusters: Ionization Potentials for Y<sub>n</sub> and Y<sub>n</sub>O ( $n = 2$ –231). *J. Chem. Phys.* **1995**, *102*, 1–5.
- (16) Reed, Z. D.; Duncan, M. A. Photodissociation of Yttrium and Lanthanum Oxide Cluster Cations. *J. Phys. Chem. A* **2008**, *112*, 5354–5362.

- (17) Dai, B.; Deng, K.; Yang, J. A Theoretical Study of the Y<sub>4</sub>O Cluster. *Chem. Phys. Lett.* **2002**, *364*, 188–195.
- (18) Gu, G.; Dai, B.; Ding, X.; Yang, J. A Theoretical Study of the Y<sub>3</sub>O Clusters. *Eur. Phys. J. D* **2004**, *29*, 27–31.
- (19) Yang, Z.; Xiong, S.-J. Structural, Electronic, and Magnetic Properties of Y<sub>n</sub>O ( $n = 2 - 14$ ) Clusters: Density Functional Study. *J. Chem. Phys.* **2008**, *129*, 124308 (7 pages).
- (20) Yang, Z.; Xiong, S.-J. Structural, Electronic and Magnetic Properties of Small Yttrium Trioxide Clusters from Density Functional Calculations. *J. Phys. B: At. Mol. Opt. Phys.* **2009**, *42*, 245101 (6 pages).
- (21) Kresse, G.; Furthmüller, J. Efficient Iterative Schemes for Ab Initio Total-Energy Calculations Using a Plane-Wave Basis Set. *Phys. Rev. B* **1996**, *54*, 11169–11186.
- (22) Vienna *ab initio* Simulation Package (VASP), Technische Universität Wien, 1999.
- (23) Perdew, J. P.; Burke, K.; Ernzerhof, M. Generalized Gradient Approximation Made Simple. *Phys. Rev. Lett.* **1996**, *77*, 3865–3868.
- (24) Blöchl, P. E. Projector Augmented-Wave Method. *Phys. Rev. B* **1994**, *50*, 17953–17979.
- (25) Kresse, G.; Joubert, D. From Ultrasoft Pseudopotentials to the Projector Augmented-Wave Method. *Phys. Rev. B* **1999**, *59*, 1758–1775.
- (26) Rahane, A. B.; Deshpande, M. D. Structural and Electronic Properties of Neutral and Ionic (Ga<sub>2</sub>O<sub>3</sub>)<sub>n</sub> Clusters with ( $n = 1 - 10$ ). *J. Phys. Chem. C* **2012**, *116*, 2691–2701.
- (27) Zhao, G. F.; Zhang, J.; Jing, Q. A Density Functional Study of Y<sub>n</sub>Al ( $n = 1 - 14$ ) Clusters. *J. Chem. Phys.* **2007**, *127*, 234312 (7 pages).
- (28) Yuan, H. K.; Chen, H.; Kuang, A. L.; Ahmed, A. S.; Xiong, Z. H. Density-Functional Calculations of the Structure and Electronic and Magnetic Properties of Small Yttrium Clusters Y<sub>n</sub> ( $n = 2 - 17$ ). *Phys. Rev. B* **2007**, *75*, 174412 (11 pages).
- (29) Humphrey, W.; Dalke, A.; Schulten, K. VMD: Visual Molecular Dynamics. *J. Mol. Graph.* **1996**, *14*, 33–38.
- (30) Monkhorst, H. J.; Pack, J. D. Special Points for Brillouin-Zone Integrations. *Phys. Rev. B* **1976**, *13*, 5188–5192.
- (31) Halevy, I.; Carmon, R.; Winterrose, M. L.; Yeheskel, O.; Tiferet, E.; Ghose, S. Pressure-Induced Structural Phase Transitions in Y<sub>2</sub>O<sub>3</sub> Sesquioxide. *J. Phys.: Conf. Ser.* **2010**, *215*, 012003 (8 pages).
- (32) Riello, P.; Fagherazzi, G.; Clemente, D.; Canton, P. X-ray Rietveld Analysis with a Physically Based Background. *J. Appl. Crystallogr.* **1995**, *28*, 115–120.
- (33) Belonoshko, A. B.; Gutierrez, G.; Ahuja, R.; Johansson, B. Molecular Dynamics Simulation of the Structure of Yttria Y<sub>2</sub>O<sub>3</sub> Phases Using Pairwise Interactions. *Phys. Rev. B* **2001**, *64*, 184103 (8 pages).
- (34) Chen, J.; Xu, Y.; Chen, D.-Q.; Zhang, J.-L. Ab Initio Study of a Y-Doped Σ31 Grain Boundary in Alumina. *Sci. China Ser. G-Phys. Mech. Astron.* **2008**, *51*, 1607–1615.
- (35) Wang, C. M.; Cargill, G. S., III; Chan, H. M.; Harmer, M. P. Structural Features of Y-Saturated and Supersaturated Grain Boundaries in Alumina. *Acta. Mater.* **2000**, *48*, 2579–2591.
- (36) Ching, W.-Y.; Xu, Y.-N.; Rühle, M. Ab-Initio Calculation of Yttrium Substitutional Impurities in α-Al<sub>2</sub>O<sub>3</sub>. *J. Am. Ceram. Soc.* **1997**, *80*, 3199–3204.
- (37) Ching, W.-Y. Electronic Structure and Bonding of All Crystalline Phases in the Silica-Silicon Nitride Phase Equilibrium Diagram. *J. Am. Ceram. Soc.* **2004**, *87*, 1996–2013.
- (38) Galmarini, S.; Aschauer, U.; Bowen, P.; Parker, S. C. Atomistic Simulation of Y-Doped α-Alumina Interfaces. *J. Am. Ceram. Soc.* **2008**, *91*, 3643–3651.
- (39) Dai, D. G.; Balasubramanian, K. Electronic States of Y<sub>n</sub> ( $n = 24$ ). *J. Chem. Phys.* **1993**, *98*, 7098–7106.
- (40) Ding, X.-L.; Li, Z.-Y.; Meng, J.-H.; Zhao, Y.-X.; He, S.-G. Density-Functional Global Optimization of (La<sub>2</sub>O<sub>3</sub>)<sub>n</sub> Clusters. *J. Chem. Phys.* **2012**, *137*, 214311 (7 pages).
- (41) Rienstra-Kiracofe, J. C.; Tschumper, G. S.; Schaefer, H. F., III; Nandi, S.; Ellison, G. B. Atomic and Molecular Electron Affinities: Photoelectron Experiments and Theoretical Computations. *Chem. Rev.* **2002**, *102*, 231–282.
- (42) Gowtham, S.; Deshpande, M.; Costales, A.; Pandey, R. Structural, Energetic, Electronic, Bonding, and Vibrational Properties of Ga<sub>3</sub>O, Ga<sub>3</sub>O<sub>2</sub>, Ga<sub>3</sub>O<sub>3</sub>, Ga<sub>2</sub>O<sub>3</sub>, and GaO<sub>3</sub> Clusters. *J. Phys. Chem. B* **2005**, *109*, 14836–14844.
- (43) Tang, W.; Sanville, E.; Henkelman, G. A Grid-Based Bader Analysis Algorithm without Lattice Bias. *J. Phys.: Condens. Matter* **2009**, *21*, 084204 (7 pages).
- (44) Ching, W.-Y.; Xu, Y.-N. Electronic and Optical Properties of Yttria. *Phys. Rev. Lett.* **1990**, *65*, 895–898.